Planning and Control for Cooperative Manipulation and Transportation with Aerial Robots

Jonathan Fink, Nathan Michael, Soonkyum Kim, and Vijay Kumar

Abstract. We consider the problem of controlling multiple robots manipulating and transporting a payload in three dimensions via cables. Individual robot control laws and motion plans enable the control of the payload (position and orientation) along a desired trajectory. We address the fact that robot configurations may admit multiple payload equilibrium solutions by developing constraints for the robot configuration that guarantee the existence of a unique payload pose. Further, we formulate individual robot control laws that enforce these constraints and enable the design of non-trivial payload motion plans. Finally, we propose two quality measures for motion plan design that minimize individual robot motion and maximize payload stability along the trajectory. The methods proposed in the work are evaluated on a team of aerial robots in experimentation.

1 Introduction

Aerial transport of payloads by towed cables is common in emergency response, industrial, and military applications for object transport to environments inaccessible by other means. Examples of aerial towing range from emergency rescue missions where individuals are lifted from dangerous situations to the delivery of heavy equipment to the top of a tall building. Typically, aerial towing is accomplished via a single cable attached to a payload. However, only limited controllability of the payload is achievable with a single attachment point [9].

In this work we consider the problem of cooperative aerial manipulation. Unlike aerial towing, which addresses the issue of controlling a point-model payload, aerial manipulation considers the control of a payload with six degrees of freedom. The cooperative aerial manipulation problem can be shown to be analogous to

Jonathan Fink · Nathan Michael · Soonkyum Kim · Vijay Kumar
GRASP Laboratory, University of Pennsylvania, Philadelphia, PA
e-mail: {jonfink,nmichael,soonkyum,kumar}@grasp.upenn.edu

C. Pradalier, R. Siegwart, and G. Hirzinger (Eds.): Robotics Research, STAR 70, pp. 643–659.
springerlink.com © Springer-Verlag Berlin Heidelberg 2011

cable-actuated parallel manipulators in three dimensions, where in the former the payload pose is affected by robot positions and in the latter pose control is accomplished by varying the lengths of multiple cable attachments. The analysis of the mechanics of cable-driven parallel manipulators is a special case of the analysis of the general problem of payloads suspended by n cables in three dimensions. The $n = 6$ case is addressed in the literature on cable-actuated payloads, where the payload pose is fully specified. When $n = 5$, if the line vectors are linearly independent and the cables are taut, the line vectors and the gravity wrench axis must belong to the same linear complex [5]. The payload is free to instantaneously twist about the reciprocal screw axis. When $n = 4$, under similar assumptions on linear independence and positive tension, the line vectors and the gravity wrench must belong to the same linear congruence. The unconstrained freedoms correspond (instantaneously) to a set of twists whose axis lie on a cylindroid. The $n = 3$ case admits solutions where all three cables and the gravity wrench axis lie on the same regulus - the generators of a hyperboloid which is a ruled surface [10].

Of note are the unilateral constraints imposed by cables that can only admit positive forces. As the tension on a cable can only be positive and the distance between the two end-points of a cable cannot be more than its free length, and further the tension is non-zero only when the distance is equal to the free lengths – each cable introduces a *complementarity constraint* of the type:

$$s \geq 0, \quad \lambda \geq 0, \quad \lambda s = 0 \tag{1}$$

where s is the slack in the cable and λ is the tension in the cable. The solutions to systems of linear equations subject to such constraints, the so-called *Linear Complementarity Problem* (LCP), have been studied extensively [3]. Even though all the terms in the LCP are linear in the unknowns, the system can have multiple solutions or no solutions at all.

In prior work, we formulated the mechanics of aerial manipulation (reviewed in Sect. 2) [7]. We focused this development for an under-actuated system with three robots and presented pose control of a payload to a sequence of desired poses. Our prior work did not address a significant challenge resulting from the under-actuation which is of great relevance when considering the problem of planning non-trivial manipulation tasks: the fact that for a given robot configuration, the physical system may admit multiple payload equilibrium solutions.

In this paper, we build upon our prior work to develop individual robot control laws and motion plans that permit the control of the payload along a desired trajectory. We address the fact that robot configurations may admit multiple payload equilibrium solutions by developing constraints for the robot configuration that guarantee the existence of a unique payload pose. We formulate individual robot control laws that enforce these constraints and enable the design of non-trivial payload motion plans.

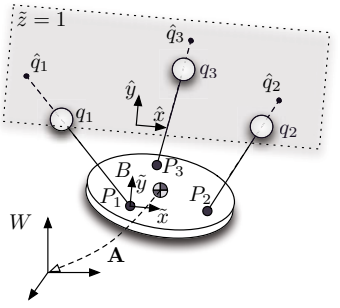

Fig. 1 A team of three point-model robots manipulate a payload in three dimensions. The coordinates of the robots in the inertial frame W are $q_i = [x_i, y_i, z_i]$ and in the body-fixed frame (attached to the payload) B are $\tilde{q}_i = [\tilde{x}_i, \tilde{y}_i, \tilde{z}_i]$. The rigid body transformation from the payload body frame aligned at the center of mass to W is $\mathbf{A} \in SE(3)$. Additionally, we denote the projection of the robot position $\tilde{q}_i$ along $q_i - p_i$ to the plane $\tilde{z} = 1$ as $\hat{q}_i = [\hat{x}_i, \hat{y}_i, 1]$.

2 Mechanics of Cooperative Manipulation

2.1 Model

We begin by considering the problem with three robots in three dimensions carrying an object (although the analysis readily extends to n robots). We consider point-model robots for the mathematical formulation and algorithmic development although the experimental implementation requires us to consider the full twelve-dimensional state-space of each quadrotor and a formal approach to realizing these point-model abstractions, which we provide in Sect. 6.1. Thus, our configuration space is given by $\mathscr{Q} = \mathbb{R}^3 \times \mathbb{R}^3 \times \mathbb{R}^3$. Each robot is modeled by $q_i \in \mathbb{R}^3$ with coordinates $q_i = [x_i, y_i, z_i]^{\mathrm{T}}$ in an inertial frame, W (Fig. 1). Define the robot configuration as $q = [q_1, q_2, q_3]^{\mathrm{T}}$. The i^{th} robot cable with length l_i is connected to the payload at the point P_i with coordinates $p_i = \left[x_i^p, y_i^p, z_i^p\right]^{\mathrm{T}}$ in W. Let $p = [p_1, p_2, p_3]^{\mathrm{T}}$ denote all attachment points. We require P_1, P_2, and P_3 to be non-collinear and span the center of mass. The payload has mass m with the center of mass at C with position vector $r = [x_C, y_C, z_C]^{\mathrm{T}}$. We denote the fixed Euclidean distance between attachment points P_i and P_j as $r_{i,j}$. The payload's pose $\mathbf{A} \in SE(3)$ can be locally parameterized using the components of the vector r and the Euler angles with six coordinates: $[x_C, y_C, z_C, \alpha, \beta, \gamma]^{\mathrm{T}}$. The homogeneous transformation matrix describing the pose of the payload is given by:

$$\mathbf{A} = \begin{bmatrix} \mathbf{R}(\alpha, \beta, \gamma) & \begin{pmatrix} x_C \\ y_C \\ z_C \end{pmatrix} \\ 0 \quad 0 \quad 0 & 1 \end{bmatrix}. \tag{2}$$

Note that $\mathbf{R}$ is the rotation matrix going from the object frame B to the world frame W (as depicted in Fig. 1). Additionally, for this work we follow the *Tait-Bryan* Euler angle parameterization for $\{\alpha, \beta, \gamma\}$.

The equations of static equilibrium can be written as follows. The cables exert zero-pitch wrenches on the payload which take the following form after normalization:

$$\mathbf{w}_i = \frac{1}{l_i} \begin{bmatrix} q_i - p_i \\ p_i \times (q_i - p_i) \end{bmatrix}.$$

The gravity wrench takes the form:

$$\mathbf{g} = -mg \begin{bmatrix} e_3 \\ r \times e_3 \end{bmatrix},$$

where g is the acceleration due to gravity and $e_3 = [0, 0, 1]^{\mathrm{T}}$. For static equilibrium:

$$\mathbf{W}\,\lambda = \begin{bmatrix} \mathbf{w}_1 & \mathbf{w}_2 & \mathbf{w}_3 \end{bmatrix} \begin{bmatrix} \lambda_1 \\ \lambda_2 \\ \lambda_3 \end{bmatrix} = -\mathbf{g} \tag{3}$$

where $\lambda_i \geq 0$ is the tension in the i^{th} cable.

In order for (3) to be satisfied (with or without non-zero tensions), the four line vectors or zero pitch wrenches, $\mathbf{w}_1$, $\mathbf{w}_2$, $\mathbf{w}_3$, and $\mathbf{g}$ must belong to the same *regulus*. The lines of a regulus are points on a 2-plane in $\mathbb{PR}^5$ [11], which implies that the body is under constrained and has three degrees of freedom. Instantaneously, these degrees of freedom correspond to twists in the *reciprocal screw system* that are reciprocal to $\mathbf{w}_1$, $\mathbf{w}_2$, and $\mathbf{w}_3$. They include zero pitch twists (pure rotations) that lie along the axes of the *complementary regulus* (the set of lines each intersecting all of the lines in the original regulus). Geometrically, (3) simply requires the gravity wrench to be reciprocal to the reciprocal screw system, a fact that will be exploited in our calculations in the next section.

We will make the following simplifying assumptions:

1. The payload is a homogeneous, planar object and the center of mass lies in the plane of the attachment points.
2. The robots are positioned initially on one side of the plane of the attachment points.
3. The mass of the object is sufficiently small that three robots are able to lift the object.
4. The system is quasi-static and we may neglect the transients associated with the payload converging to an equilibrium position.

For the analysis, we will use a local frame, B, attached to the payload that is defined with the origin at P_1, the x axis pointing toward P_2 and the $x-y$ plane coincident with the plane formed by P_1, P_2, and P_3. In this local coordinate system, the components are denoted by $\tilde{(\cdot)}$ and given as:

$$P_1 = [0,0,0]^{\mathrm{T}}, \qquad P_2 = [\tilde{x}_2^p, 0, 0]^{\mathrm{T}}, \qquad P_3 = [\tilde{x}_3^p, \tilde{y}_3^p, 0]^{\mathrm{T}};$$
$$\tilde{q}_1 = [\tilde{x}_1, \tilde{y}_1, \tilde{z}_1]^{\mathrm{T}}, \qquad \tilde{q}_2 = [\tilde{x}_2, \tilde{y}_2, \tilde{z}_2]^{\mathrm{T}}, \qquad \tilde{q}_3 = [\tilde{x}_3, \tilde{y}_3, \tilde{z}_3]^{\mathrm{T}}.$$

Note that without loss of generality, we assume that $\tilde{x}_2^P > \tilde{x}_3^P$, restricting the possible permutations of P_i.

2.2 Kinematics

In this section, we determine the pose of the payload for given positions of the quadrotors (the direct problem) and the positioning of the quadrotors for a desired pose of the payload (the inverse problem). The direct and inverse problems are analogous to the direct and inverse kinematics for manipulators. However, they are different in that one must incorporate the equations of static equilibrium in order to determine the answer.

2.2.1 The Direct Problem

With hovering robots and cables in tension, we can treat the object as being attached to three stationary points through rigid rods and ball joints to arrive at the constraints

$$\|q_i - p_i\| = l_i, \tag{4}$$

for $i = \{1,2,3\}$. In addition, we impose the three equations of static equilibrium, (3), to further constrain the solutions.

Problem 1 (Direct Problem). Given the positions of the robots, q_i, $i = \{1,2,3\}$, find the position(s) and orientation(s) of the payload satisfying the kinematics of the robots-cables-payload system (4) and the equations of equilibrium (3).

We solve this problem by finding the three screws (twists) that are reciprocal to the three zero pitch wrenches. Define the 6×3 matrix $\mathbf{S}$ of twists with three linearly independent twists such that the vectors belong to the null space of $\mathbf{W}^{\mathrm{T}}$:

$$\mathbf{W}^{\mathrm{T}}\mathbf{S} = 0.$$

$\mathbf{S}$ is an algebraic function of the positions of the three pivot points, P_i. In order to satisfy (3), p_i must satisfy the three algebraic conditions:

$$\mathbf{S}(x_i^P, y_i^P, z_i^P)^{\mathrm{T}}\mathbf{g} = 0. \tag{5}$$

Finally, we require that there exist a *positive*, 3×1 vector of multipliers, λ, that satisfies (3). We find the multipliers using the Moore-Penrose inverse, $\mathbf{W}^{\dagger}$, of $\mathbf{W}$,

$$\lambda = -\mathbf{W}^{\dagger}\mathbf{g},$$

This allows us to eliminate equilibrium poses corresponding to tensions that violate the non-negativity constraints on the multipliers.

Thus, the direct problem reduces to solving (4, 5). Accordingly, the object has three degrees of freedom. Imposing the three equilibrium conditions in (5) we can, in principle, determine a finite number of solutions for this analog of the direct kinematics problem.

2.2.2 The Inverse Problem

The inverse problem reduces to the problem of solving for the three-dimensional set $Q_c \subset \mathcal{Q}$ by solving for the nine variables $\{(\tilde{x}_i, \tilde{y}_i, \tilde{z}_i), i = 1, 2, 3\}$ subject to (4, 5).

Problem 2 (Inverse Problem). Given the desired payload position and orientation (2), find positions of the robots (q_i) that satisfy the kinematics of the robots-cables-payload system and the equations of equilibrium (3).

We now restrict our attention to a reduced space of possible configurations based upon the assumptions $(1, 2)$. We introduce the notion of normalized components, denoted by $(\hat{\cdot})$, with $\hat{q}_i = [\hat{x}_i, \hat{y}_i, 1]$ to define the position of the i^{th} robot projected to a constant height $\tilde{z}_i = 1$ above the payload. Based on this simplification (we now only need to solve for three planar positions), we redefine the static equilibrium condition as

$$\mathbf{S}(\hat{x}_i, \hat{y}_i, 1)^{\mathrm{T}}\tilde{\mathbf{g}} = 0. \tag{6}$$

Solving the system of equations in (6) yields algebraic solutions for $\{\hat{x}_2, \hat{x}_3, \hat{y}_3\}$ as functions of $\{\hat{x}_1, \hat{y}_1, \hat{y}_2\}$. Note that any solution to (6) is indeed a solution to (5). Further, we may compute the position of the robots $\tilde{q}_i$ given the normalized coordinates $\hat{q}_i$ and the kinematic constraint (4) as

$$\tilde{q}_i = l_i \frac{\hat{q}_i}{\|\hat{q}_i\|} + P_i.$$

By using $\hat{q}_i$ as coordinates, we can obtain closed-form analytic solutions for the positions of all robots that respect the kinematic constraints and the condition for static equilibrium.

3 Solving the Direct Problem

In this section, we consider an optimization-based formulation to determining solutions to the direct problem. We begin by stating the optimization problem that minimizes the potential energy of the rigid payload.

Problem 3 (Optimization-Based Formulation of the Direct Problem)

$$\begin{aligned} \min_{p_i} \quad & z_1^p + z_2^p + z_3^p \\ \text{s.t.} \quad & \|q_i - p_i\| \le l_i, \quad i = \{1, 2, 3\} \\ & \|p_i - p_j\| = r_{i,j}, \quad i, j = \{1, 2, 3\}, i \neq j. \end{aligned}$$

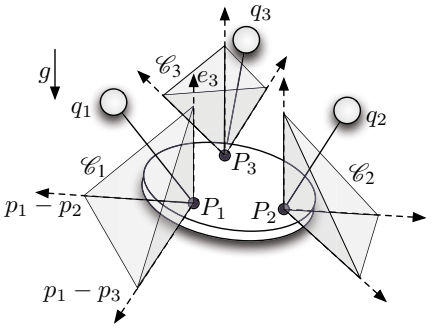

Fig. 2 A graphical depiction of the cone constraints presented in Proposition 1.

We have replaced the equations of static equilibrium for cables in tension, (4), with inequalities (a more accurate restatement of Problem 1). The minimization in Problem 3 explicitly prohibits local maxima while ensuring $\lambda_i \geq 0$, allowing for $\lambda_i = 0$ (the i^{th} cable becoming slack) as modeled in the complementarity constraints (1).

Problem 3 is non-convex due to the payload rigidity, which shows up as the equality constraint $\|p_i - p_j\| = r_{i,j}$. However, by relaxing this condition, we see that the program becomes convex.

Problem 4 (Convex Formulation of the Relaxed Direct Problem)

$$\begin{aligned} \min_{p_i} \quad & z_1^p + z_2^p + z_3^p \\ \text{s.t.} \quad & \|q_i - p_i\| \leq l_i, \quad i = \{1,2,3\} \\ & \|p_i - p_j\| \leq r_{i,j}, \quad i,j = \{1,2,3\}, i \neq j. \end{aligned}$$

Clearly, this formulation relaxes the rigidity requirement of the payload. However, the problem of solving for the equilibrium pose of the payload is now a Second Order Cone Program (SOCP) [6] and convex.

We now seek conditions on robot positions that enforce the rigidity of the payload while preserving the structure of the SOCP in Problem 4.

Proposition 1 (Conditions for Unique Solutions to the Direct Problem). *The solution to Problem 3 is unique provided that $q_i - p_i$ lies strictly inside the convex cone $\mathscr{C}_i$, defined by the vectors $(p_i - p_j)$, $(p_i - p_k)$, and e_3 $(j \neq i, k \neq i, j \neq k)$, where $e_3 = [0,0,1]^T$.*

Proof. We begin by considering the SOCP in Problem 4. The First Order Necessary Conditions (FONC) are:

$$\begin{aligned} \mu_1(p_1 - q_1) + \mu_4(p_1 - p_2) + \mu_6(p_1 - p_3) + \frac{1}{2}e_3 = 0 \\ \mu_2(p_2 - q_2) + \mu_4(p_2 - p_1) + \mu_5(p_2 - p_3) + \frac{1}{2}e_3 = 0 \\ \mu_3(p_3 - q_3) + \mu_5(p_3 - p_2) + \mu_6(p_3 - p_1) + \frac{1}{2}e_3 = 0 \end{aligned} \tag{7}$$

with

$$\|p_i - q_i\| \leq l_i, \quad \mu_i \geq 0, \quad \mu_i(\|p_i - q_i\|^2 - l_i^2) = 0 \quad \text{for} \quad i = \{1, 2, 3\},$$

and

$$\begin{aligned}
\|p_1 - p_2\| &\leq r_{1,2}, \quad \mu_4 \geq 0, \quad \mu_4(\|p_1 - p_2\|^2 - r_{1,2}^2) = 0 \\
\|p_2 - p_3\| &\leq r_{2,3}, \quad \mu_5 \geq 0, \quad \mu_5(\|p_2 - p_3\|^2 - r_{2,3}^2) = 0 \\
\|p_3 - p_1\| &\leq r_{3,1}, \quad \mu_6 \geq 0, \quad \mu_6(\|p_3 - p_1\|^2 - r_{3,1}^2) = 0.
\end{aligned}$$

Eliminating the condition when the payload is in a vertical orientation, $p_i \times p_j \cdot e_3 \neq 0$, for all $i \neq j$, from (7) it is clear that μ_1, μ_2, and μ_3 are all strictly positive. The variables μ_i correspond to forces in the physical system, with $i = \{1, 2, 3\}$ representing the cable tensions. If we can show that μ_4, μ_5, and μ_6, the three internal forces between the anchor points of the triangle, are strictly positive, the inequalities $\|p_i - p_j\| \leq r_{i,j}$ satisfy the rigidity (strict equality) requirement of Problem 3.

Consider the FONC for q_1,

$$q_1 - p_1 = \frac{\mu_4}{\mu_1}(p_1 - p_2) + \frac{\mu_6}{\mu_1}(p_1 - p_3) + \frac{1}{2\mu_1}e_3. \tag{8}$$

This equation is the force balance equation at P_1 up to a scalar multiplier. If we require that $q_1 - p_1$ lies *strictly inside* the convex cone $\mathscr{C}_1$, generated by $(p_1 - p_2)$, $(p_1 - p_3)$, and e_3:

$$q_1 - p_1 = \eta_{1,1}(p_1 - p_2) + \eta_{1,2}(p_1 - p_3) + \eta_{1,3}e_3, \tag{9}$$

with $\eta_{1,i} > 0$ for $i = \{1, 2, 3\}$, the coefficients $\frac{\mu_4}{\mu_1}$, $\frac{\mu_6}{\mu_1}$, and $\frac{1}{2\mu_1}$ must be strictly positive. A similar argument holds for q_2 and q_3 to show that μ_4, μ_5, and μ_6 are all strictly positive under this requirement.

Thus, if $q_i - p_i$ lies *strictly inside* the convex cone $\mathscr{C}_i$, the solution to the SOCP is also a solution to Problem 3. Further, as an SOCP is convex, the solution to Problem 3 is unique with the restriction on robot positions defined by (9). □

The result of Proposition 1 is a set of conditions on individual robot positions with respect to the payload that guarantee a unique solution to the direct problem (as depicted in Fig. 2). We will call the conditions $q_i - p_i \in \mathscr{C}_i$ the *cone constraints*. In the next section we develop individual robot control laws that ensure these constraints are preserved while driving the robot configuration, q, to a desired state.

4 Robot Control Laws

We begin by formulating (9) for the i^{th} robot as

$$q_i = A_i\eta_i + p_i,$$

where

$$\eta_i = \left[\eta_{i,1}, \eta_{i,2}, \eta_{i,3}\right]^{\mathrm{T}}$$

and

$$A_i = \left[p_i - p_j,\ p_i - p_k,\ e_3\right],\ j \neq i, k \neq i, j \neq k.$$

A_i is full rank and invertible, permitting the computation of η_i given the robot position q_i and payload configuration p:

$$\eta_i = A_i^{-1}(q_i - p_i). \tag{10}$$

Note that η_i is unique for any q_i and p up to a rigid body translation and rotation of the payload about e_3. Additionally, for the development that follows we treat the system as quasi-static (the fourth assumption stated in Sect. 2.1).

We wish to design control laws for individual kinematic agents, $u_i = \dot{q}_i$, that drive the full system q and p to a desired time-invariant configuration defined by q^d and p^d while respecting the cone constraints. The easiest way to guarantee convergence to a time-invariant q_i^d (and thus q^d) is to require the error, $q_i^e = (q_i^d - q_i)$, to converge exponentially to zero:

$$\dot{q}_i^\star = K_i q_i^e, \tag{11}$$

where K_i is any positive definite 3×3 matrix. From (11), we obtain robot velocities that guarantee globally asymptotic convergence to the desired robot configuration. However, due to the conditions on $\eta_{i,j}$ for the i^{th} robot with $j = \{1, 2, 3\}$, we must also consider the position of each robot with respect to the payload pose p.

We relax the requirement of exponential convergence to a desired robot configuration and replace it with a slightly different notion of convergence in order to accommodate the cone constraints. Specifically instead of insisting on (11), we find the solution closest to the velocities corresponding to the exponential solution which also enforce the cone constraints; and thus guarantee a unique solution to the direct problem.

We require that the error in the robot state decrease *monotonically*:

$$q_i^{e\mathrm{T}} K_i \dot{q}_i \geq 0, \tag{12}$$

treating K_i as a diagonal matrix. Further, from (10), we see that the cone constraints of Proposition 1 are met when $\eta_{i,j} > 0$. Therefore, we introduce active constraints that enforce this requirement when $\eta_{i,j} < \delta_{i,j}$, where $\delta_{i,j}$ is a value selected near the constraint boundary. We will require

$$\dot{\eta}_{i,j} \geq 0 \tag{13}$$

when $\eta_{i,j} < \delta_{i,j}$. Differentiating (10),

$$\dot{\eta}_{i,j} = \dot{A}_i^{-1}(q_i - p_i) + A_i^{-1}(\dot{q}_i - \dot{p}_i).$$

Recalling that $A_i A_i^{-1} = I_{3\times 3}$ and thus $\dot{A}_i A_i^{-1} = -A_i \dot{A}_i^{-1}$, (13) is equivalently written as

$$\dot{q}_i \geq \dot{A}\eta_i + \dot{p}_i. \tag{14}$$

Proposition 2 (Decentralized Robot Control Law). *Equation (15) is a decentralized control law that selects a unique control input that is instantaneously closest to*

(11) while satisfying the monotonic convergence inequality and enforcing the cone constraints.

$$\dot{q}_i = \arg\min_{\dot{\tilde{q}}_i} \|\dot{q}_i^\star - \dot{\tilde{q}}_i\|^2, \quad s.t. \quad (12,14) \tag{15}$$

Proof. The constraints in (12,14) provide the monotonic convergence condition and enforcement of the cone constraints. The function being minimized is the discrepancy from the exponentially convergent solution. Since the inequality constraints are linear in $\dot{q}_i$ and the function being minimized is a positive-definite, quadratic function of $\dot{q}_i$, (15) is a convex, quadratic program (QP) with a unique solution. Further, as each robot only relies on its own state and knowledge of the payload pose, it is a decentralized control law. □

Remark 1. The requirement of the cone constraints implies that robots will not collide. Therefore, inter-robot collision avoidance is maintained through (14) as enforced by (15).

Convergence properties of (15) To investigate the global convergence properties, we introduce the Lyapunov function

$$V(q) = \frac{1}{2} q^{e\mathrm{T}} q^e,$$

for the system of robots, q. Recalling from Proposition 1 that the enforcement of $\eta_{i,j} > 0$ implies uniqueness of p, it is sufficient to consider the convergence of q to q^d to show $p = p^d$. Since the solution of (15) must satisfy the inequality (12), we know that $q^{e\mathrm{T}} K \dot{q} \geq 0$. If K is chosen to be a diagonal 9×9 matrix with positive entries, this condition also implies $q^{e\mathrm{T}} \dot{q} \geq 0$. In other words, $\dot{V}(q) = -q^{e\mathrm{T}} \dot{q} \leq 0$. Clearly $V(q) \to \infty$ as $\|q\| \to \infty$. Further, $V(q)$ is globally uniformly asymptotically stable. Therefore, from LaSalle's invariance principle, we know that the robot configuration will converge to the largest invariant set given by $q^{e\mathrm{T}} \dot{q} = 0$. Additionally, we know that $\dot{q} = 0$ only when $\dot{q}_i = 0$ for $i = \{1, 2, 3\}$. Thus the invariant set is characterized by the set of conditions that lead to the system of inequalities given by (12, 14) to have $\dot{q}_i = 0$ as the only solution for $i = \{1, 2, 3\}$.

5 Planning for Aerial Manipulation

In this work, we take a decoupled approach to motion planning for the payload subject to the constraints of aerial manipulation. That is, we first plan a collision-free path in $SE(3)$ for a conservative approximation of the full robots-cables-payload system and then generate coordinated robot trajectories that enact that plan. Here we focus on the task of choosing robot trajectories for a given payload path.

Consider the manipulation workspace $Q_M \subset Q_c$, where Q_c is a function of the payload orientation and is computed in Sect. 2.2.2 to be the set of robot positions such that there is positive tension in each cable and the payload is in equilibrium.

Other factors that further constrain feasible robot configurations are maximum allowable tension ($\lambda_i < \lambda_{max}$) and the cone constraints ($\eta_i > 0$) presented in Proposition 1. While these constraints are easily computable, they are non-smooth in nature and generate a nontrivial workspace for planning.

As the constraints on Q_M do not reduce it to a unique solution for a given payload pose, there are in fact sets of configurations parameterized by $\{\hat{x}_1, \hat{y}_1, \hat{y}_2\}$ that can be chosen to stabilize the payload to a given orientation. The planning problem is: (a) to find feasible robot configurations at each point along the desired payload trajectory and (b) exploit the redundancy in configurations to optimize specified secondary design goals or quality measures. Examples of optimizing quality measures include minimizing the distance traveled by individual robots or maximizing the natural frequency of the robots-cables-payload system to lead to faster attenuation of disturbances.

5.1 Algorithm and Quality Measure

The motion planning problem we are considering is formalized as follows. Given a payload path specified by a series of waypoints $\{\mathbf{A}^0, \mathbf{A}^1, \ldots, \mathbf{A}^n\}$ where $\mathbf{A}^k \in SE(3)$, find a series of robot poses $\{q^0, q^1, \ldots, q^n\}$ where $q^k = \{q_1^k, q_2^k, q_3^k\} \in Q_M(\mathbf{A})$ such that the payload under the quasi-static assumption achieves the desired pose, $\mathbf{A}^k$. Since there are generally a set of feasible configurations q for a given payload pose $\mathbf{A}$ but no analytic representation of the set $Q_m(\mathbf{A})$, we use a sampling-based approach to evaluate candidate configurations. Selection of $\{\hat{x}_1, \hat{y}_1, \hat{y}_2\}$ yields a point in $Q_C(\mathbf{A})$ which is mapped to q and verified with respect to $\eta_i > 0$ and $\lambda_i < \lambda_{max}$ to be in $Q_M(\mathbf{A})$. Configurations are chosen to minimize a metric $D(q^{k+1}, q^k)$.

Since we have no formal completeness guarantees for this algorithm, we make the following assumption. The set of feasible payload configurations $\mathbf{A}_{feasible}$ such that $Q_M(\mathbf{A}_{feasible}) \neq \emptyset$ is defined by bounds on the roll and pitch angles of the payload and $Q_M(\mathbf{A}_{feasible})$ is sufficiently large that an initial feasible sample is always found. The space $Q_M(\mathbf{A})$ is explored with uniform sampling.

As with any sampling-based planning method, attention must be paid to the edges *connecting* states. In this work, we naively consider states to be connected by straight lines in Euclidean space and necessary deviations from this plan are computed by the individual robot control laws in (15).

We focus on two candidate quality measures for manipulation planning: a distance-based measure that seeks to minimize robot paths and a natural frequency-based measure that maximizes natural frequency of the payload around the stable equilibrium. For the distance-based quality measure, a candidate configuration is evaluated according to the function

$$D_{distance}(q^{k+1}, q^k) = ||q^{k+1} - q^k||.$$

The natural frequency-based quality measure is computed as

$$D_{frequency}(q^{k+1}, q^k) = -\text{eig}_0(\mathscr{H}(q^{k+1}))$$

where $\mathscr{H}(q)$ is the hessian of the potential energy as computed in [8] and $\text{eig}_0(M)$ is the smallest eigenvalue of the matrix M.

5.2 Coordinated Control

In order for the payload to follow the desired trajectory $\mathbf{A}^k$, the individual robots must follow their computed plans in a coordinated way. That is, the control of the robots along their paths must occur in $\mathbb{R}^9$. Given the piecewise linear interpolation $q(s)$ of robot waypoints q^k and a current robot configuration q, we compute an instantaneous goal for the system as $q(s^* + \Delta s)$ where $q(s^*)$ is the closest point along the path to the current configuration and Δs relates to the velocity along the path by $v_{path} = \frac{\Delta s}{\Delta t}$ where v_{path} is chosen to be small enough to maintain our quasi-static assumption. If $q(s^* + \Delta s)$ is not in Q_M, a sweep along Δs is performed to find the next feasible point (the next waypoint q^{k+1} in the worst case). The individual robot control law (15) navigates around these infeasible regions.

6 Experimentation

Here, we evaluate the individual robot control laws and motion planning strategies presented in Sects. 4-5. In the presentation that follows we study the performance of the system shown in Fig. 3 to control along desired trajectories or to desired configurations via the previously discussed methods.

The experiments are conducted with the AscTec Hummingbird quadrotor [1], from Ascending Technologies GmbH, with localization information being provided by a Vicon motion capture system [2] running at 100 Hz with millimeter accuracy. Control commands are sent to each robot via Zigbee at 20 Hz. The quadrotor is specified to have a payload capacity of 0.2 kg.

Robots are positioned inside the $6.7\,\text{m} \times 4.4\,\text{m} \times 2.75\,\text{m}$ workspace with an accuracy of approximately $\pm 0.05\,\text{m}$ in each direction. However, as the robots experience the effects of external loads and interactions during manipulation, this accuracy decreases to approximately $\pm 0.15\,\text{m}$.

The payload is a rigid frame with cable attachment points given by $\tilde{x}_2^p = 1\,\text{m}$, $\tilde{x}_3^p = 0.5\,\text{m}$, and $\tilde{y}_3^p = 0.87\,\text{m}$ with mass $m = 0.25\,\text{kg}$. Therefore, the mass of the payload is more than the payload capacity of a single robot. The cable lengths are equal with $l_i = 1\,\text{m}$.

6.1 The Quadrotor Robots

We begin by considering an aerial robot in $\mathbb{R}^3$ with mass m and position and orientation, $q = [x, y, z] \in \mathbb{R}^3$, and $\mathbf{R}(\alpha, \beta, \gamma) \in SO(3)$, respectively. We do not have direct access to the six control inputs for linear and angular force control, but instead have access to four control inputs related to these values. Therefore, we must restrict our interaction with the robot to the control inputs $\nu = [\nu_1, \ldots, \nu_4]$ defined over the intervals $[\nu_1, \nu_2, \nu_3] \in [-1, 1]$ and $\nu_4 \in [0, 1]$.

Based on system identification and hardware documentation, we assume the following transformation from the control inputs to the force control running on the robot (in the *body* frame of the robot):

$$\begin{aligned}\tau_x &= -K^q_{v,x}\dot{\alpha} - K^q_{p,x}(\alpha - \nu_1\alpha_{max})\\ \tau_y &= -K^q_{v,y}\dot{\beta} - K^q_{p,y}(\beta - \nu_2\beta_{max})\\ \tau_z &= -K^q_{v,z}\dot{\gamma} - K^q_{p,z}\nu_3\gamma_{inc}\end{aligned}$$

where τ is the torque applied by the robot in the body frame. Thrust along the z-axis in the body frame is defined as $f_z = \nu_4 f_{max}$. Through system identification, we determined values for these parameters. Therefore, in the discussion that follows, we consider the following desired inputs:

$$\left[\alpha^d, \beta^d, \gamma^d, f_z^d\right] = \left[\nu_1\alpha_{max}, \nu_2\beta_{max}, \nu_3\gamma_{inc}, \nu_4 f_{max}\right], \tag{16}$$

noting that we can compute the control inputs, ν_i, given the desired values with known parameters.

We now derive a transformation from point-model control in the world frame to the hardware-dependent control inputs, ν_i. Define the robot dynamics in the world frame, but only as a function of position ($q \in \mathbb{R}^3$), as

$$mI_3\ddot{q} = F_g + \left[F_x, F_y, F_z\right]^{\mathrm{T}}.$$

If we consider the forces applied to the system in the robot body frame,

$$\left[0, 0, f_z\right] = \left[F_x, F_y, F_z\right]\mathbf{R}(\alpha, \beta, \gamma), \tag{17}$$

we find a well-posed equation for α, β, and f_z given the current γ and forces F_x, F_y, and F_z in the world frame. Solving the system in (17), considering that $f_z \geq 0$ and physical system performance, yields a piece-wise smooth function such that we may define a force F in the world frame that is transformed into appropriate control input via (16) (see [7] for further details). To this end, we compute these values in implementation based on proportional-integral-derivative (PID) feedback control laws determined by the desired robot positions and velocities. For the purposes of this work, we additionally control $\gamma = 0$.

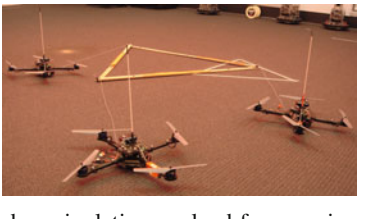

Fig. 3 The aerial robots and manipulation payload for experimentation. The payload is defined by $m = 0.25\,\mathrm{kg}$ and $\tilde{x}_2^p = 1\,\mathrm{m}$, $\tilde{x}_3^p = 0.5\,\mathrm{m}$, and $\tilde{y}_3^p = 0.87\,\mathrm{m}$, with $l_i = 1\,\mathrm{m}$.

6.2 Results

Here we present three specific examples of aerial manipulation. The first highlights the manipulation of the payload along a complex trajectory. The second considers the effect of different quality measures on planning robot configurations. The final evaluation studies the capability of the control laws to maintain cone constraints when necessary. A *C* implementation of the SOCP allows us to solve the direct problem and efficiently construct and validate complex motion plans for the robots given a desired payload trajectory. Given these motion plans, we compute individual robot controls (15) via a *C++* QP solver [4] to follow the desired trajectory with a 20 Hz update rate.

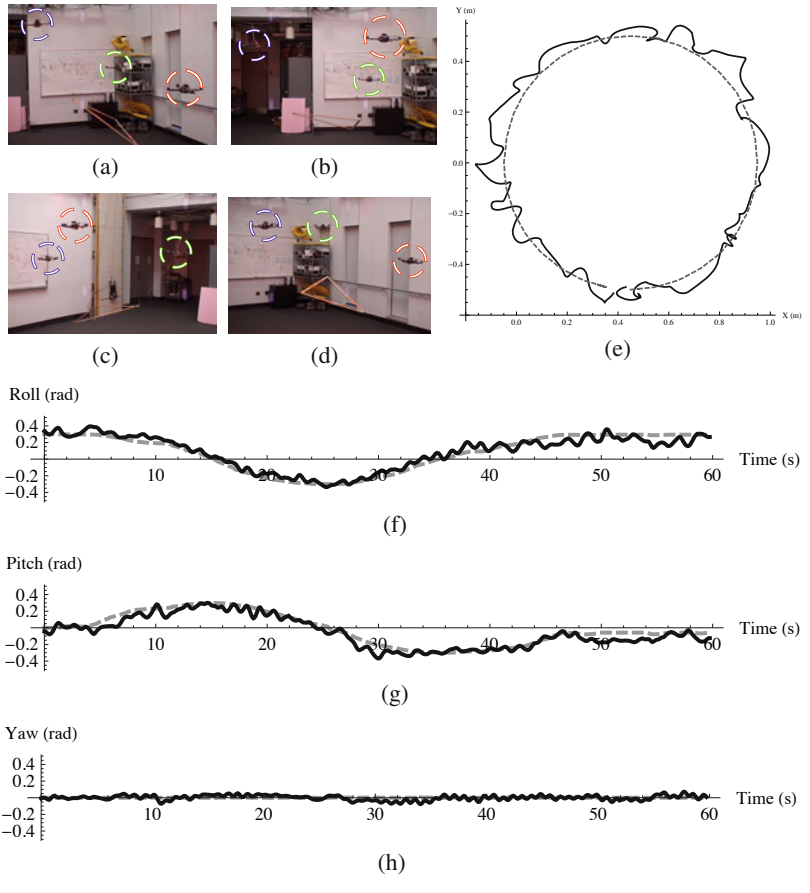

Fig. 4 Pose of the payload while being manipulated along the circular trajectory of Sect. 6.2.1. Figures 4(a)–4(d) are snapshots from an experimental trial. The robots control the payload in experimentation (solid line) along a desired trajectory (dashed line) (Figs. 4(e)–4(h)). A video of a trial run is available at http://kumar.cis.upenn.edu/movies/ISRR2009.flv

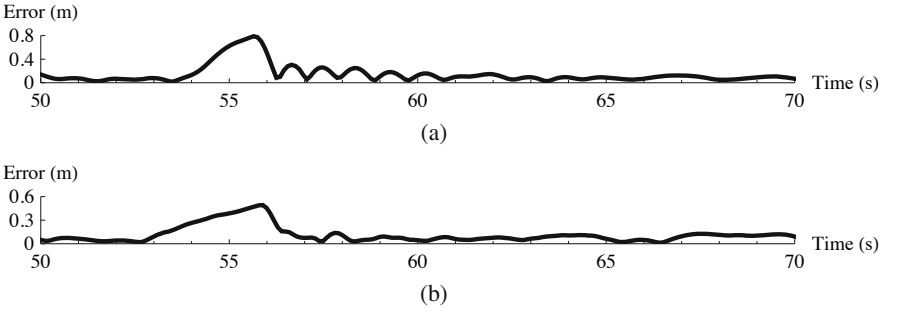

Fig. 5 A disturbance is applied to the payload at time 55 s. Notice that the configuration in Fig. 5(b), chosen to maximize natural frequency, attenuates error more quickly than the configuration in Fig. 5(a) where robot motions are minimized.

6.2.1 Trajectory Control

Depicted in Figs. 4(a)–4(d), this trial consist of a circular trajectory defined for the payload center of mass with varying roll and pitch such that

$$x_c(\theta) = 0.5\sin(\theta) + 0.45, \quad y_c(\theta) = 0.5\cos(\theta), \quad z_c = 1.0,$$
$$\alpha(\theta) = 0.3\cos(\theta), \quad \beta(\theta) = 0.3\sin(\theta), \quad \gamma = 0.$$

The motion plan is generated with $\theta = n\pi/16$ for $n = \{0, \ldots, 32\}$ using the $D_{distance}$ metric that seeks to minimize the distance traveled by the robots.

Figures 4(e)–4(h) depict the trajectory followed by the payload and the control error of the robots following their planned trajectories. In this trial, a root-mean-square (RMS) error on robot control of approximately 9 cm yields RMS error on the payload of 7 cm for the center of mass and 3° for the orientation. We have observed similar robot control and payload error over many trials as detailed in Table 1. Each waypoint in the motion plan is selected to satisfy equilibrium conditions and maximum tension and cone constraints.

6.2.2 Effect of Planning Quality Measure

In this test, the payload is carried along a translational trajectory designed with both $D_{distance}$ and $D_{frequency}$. During transport, an external disturbance is applied to the payload and we observe the response. Figure 5 depicts the behavior of the motion plans for each measure and shows that the system configuration determined by the natural frequency-based measure attenuates payload error more quickly than the equivalent configuration specified by the distance-based measure.

6.2.3 Non-trival Waypoint Navigation

For a final experimental evaluation, we demonstrate the utility of the individual robot control laws for navigation between two waypoints when the straight-line

Table 1 RMS error of robot positions and payload position and orientation as compared to the desired robot-payload configuration. Note that the sixth trial corresponds to Fig. 4.

Trial	1	2	3	4	5	6
Robot Error (m)	0.095	0.102	0.106	0.103	0.098	0.087
Payload Center of Mass Error (m)	0.075	0.087	0.084	0.089	0.086	0.067
Payload Orientation Error (deg)	4.13	3.95	4.32	3.74	4.05	2.89

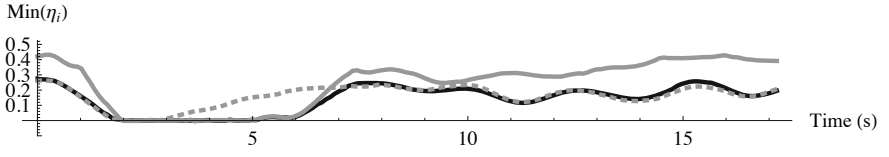

Fig. 6 Robot velocities are chosen to maintain $\eta_i > 0$ via the individual robot control law (15).

interpolated path is not feasible. The trial consists of desired waypoints requiring a rotation of the system by 120° about e_3. Figure 6 shows that the cone constraints are maintained throughout the trial and illustrates in areas of free-space that the planner need only focus on gross motions of the payload and robot configurations at the endpoints as the online controller will find the constraint-free robot trajectories.

7 Conclusion and Future Work

We presented individual robot control laws and motion plans that permit the control of the payload along a desired trajectory. We address the fact that robot configurations may admit multiple payload equilibrium solutions by developing constraints for the robot configuration that guarantee the existence of a unique payload pose. We formulate individual robot control laws that enforce these constraints and enable the design of non-trivial payload motion plans. We propose two quality measures for motion plan design that minimize individual robot motion and maximize payload stability along the trajectory. The methods proposed in this work are evaluated on a team of aerial robots in experimentation.

We are currently addressing limiting factors relating to system performance including the rate and effects of sensing and actuation errors on the control of the robots. To this end, we are implementing on-board estimation and control methods that consider the stochasticity of the system, increase control rates, and reduce our reliance on global localization. Additionally, we are exploring the limitations of the quasi-static assumption and the effect of transients on our individual robot control laws.

References

1. Ascending Technologies, GmbH, http://www.asctec.de
2. Vicon Motion Systems, Inc., http://www.vicon.com
3. Cottle, R.W., Pang, J., Stone, R.E.: The Linear Complementarity Problem. Academic Press, London (1992)
4. Fischer, K., Gartner, B., Schonherr, S., Wessendorp, F.: Linear and quadratic programming solver. In: Board, C.E. (ed.) CGAL User and Reference Manual (2007)
5. Hunt, K.: Kinematic Geometry of Mechanisms. Oxford University Press, Oxford (1978)
6. Lobo, M.S., Vandenberghe, L., Boyd, S., Lebret, H.: Application of second-order cone programming. Linear Algebra and Its Applications 284, 192–228 (1998)
7. Michael, N., Fink, J., Kumar, V.: Cooperative manipulation and transportation with aerial robots. In: Robotics: Science and Systems, Seattle, WA (2009)
8. Michael, N., Kim, S., Fink, J., Kumar, V.: Kinematics and statics of cooperative multi-robot aerial manipulation with cables. In: ASME Int. Design Engineering Technical Conf. & Computers and Information in Engineering Conf., San Diego, CA (2009) (to appear)
9. Murray, R.M.: Trajectory generation for a towed cable system using differential flatness. In: IFAC World Congress, San Francisco, CA (1996)
10. Phillips, J.: Freedom in Machinery, vol. 1. Cambridge University Press, Cambridge (1990)
11. Selig, J.M.: Geometric Fundamentals of Robotics. Springer, Heidelberg (2005)